

Growth Factors, Cytokines, Cell Cycle Molecules

# The CC Chemokine Ligand, CCL2/MCP1, Participates in Macrophage Fusion and Foreign Body Giant Cell Formation

Themis R. Kyriakides,\* Matt J. Foster,\*  
Grant E. Keeney,\* Annabel Tsai,†  
Cecilia M. Giachelli,† Ian Clark-Lewis,‡  
Barrett J. Rollins,§ and Paul Bornstein\*

From the Departments of Biochemistry\* and Bioengineering,†  
University of Washington, Seattle, Washington; the Department of  
Biochemistry and Molecular Biology,‡ University of British  
Columbia, Vancouver, Canada, and the Dana Farber Cancer  
Institute,§ Harvard Medical School, Boston, Massachusetts

**The foreign body reaction (FBR) develops in response to the implantation of almost all biomaterials and can be detrimental to their function. The formation of foreign body giant cells (FBGC), which damage the surface of biomaterials, is considered a hallmark of this reaction. FBGC derive from blood-borne monocytes that enter the implantation site after surgery in response to the release of chemotactic signals. In this study, we implanted biomaterials subcutaneous (s.c.) in mice that lack the monocyte chemoattractant CC chemokine ligand 2 (CCL2) and found that biomaterials were encapsulated despite reduced FBGC formation. The latter was due to compromised macrophage fusion rather than migration. Consistent with the reduction in FBGC formation, biodegradable biomaterials sustained reduced damage in CCL2-null mice. Furthermore, blockade of CCL2 function by localized gene delivery in wild-type mice hindered FBGC formation, despite normal monocyte recruitment. The requirement for CCL2 in fusion was confirmed by the ability of both a CCL2 inhibitory peptide and an anti-CCL2 Ab to reduce FBGC formation from peripheral blood monocytes in an *in vitro* assay. Our findings demonstrate a previously unreported involvement of CCL2 in FBGC formation, and suggest that FBGC are not the primary determinants of capsule formation in the FBR. (Am J Pathol 2004, 165:2157–2166)**

Implantation of biomaterials and tissue-engineered devices into tissues leads to the development of a foreign

body reaction (FBR) that can cause implant failure.<sup>1,2</sup> The FBR has been implicated in the malfunction and failure of numerous devices and implants.<sup>3–6</sup> This is due to the unavoidable remodeling of the implant and the implantation site. However, to date the molecular signals that regulate the development of the FBR have not been defined. At the cellular level we know that, shortly after implantation, phagocytic neutrophils are recruited to the site and serve as the initial line of defense. The second wave of defense is dominated by monocytes that extravasate into the implantation site and differentiate into macrophages. In normal wound healing the accumulation of neutrophils and activated macrophages is transient and gives way to the proliferation and remodeling phases that complete wound repair.<sup>7</sup> On the contrary, in the foreign body response, macrophages persist at the site of implantation and frequently undergo fusion to generate multinucleated giant cells.<sup>8</sup> These cells, known as foreign body giant cells (FBGC), are unique to the FBR and are present exclusively at the tissue-implant interface. FBGC are believed to be key mediators of the inflammatory response. In addition, due to the large surface area of the biomaterial they can occupy, FBGC can create high concentrations of enzymes that can cause extensive surface damage.<sup>9</sup> Furthermore, due to their phagocytic activity, FBGC can generate particulate debris that can contribute to the persistence of inflammation. Eventually, due to the FBR, implanted biomaterials become encapsulated by a collagenous, largely avascular, capsule within 2 to 4 weeks following implantation.

Macrophages are recruited to the site of implantation as blood-borne monocytes in response to signals from other inflammatory cells such as neutrophils, and become activated *in situ*. The exact nature of such signals has not been elucidated, but reports indicate that they

Supported by the University of Washington Engineered Biomaterials Engineering Research Center (National Science Foundation grant EEC9529161) and National Institutes of Health grant AR 45418.

Accepted for publication September 7, 2004.

Address reprint requests to Themis R. Kyriakides, Department of Pathology and Biomedical Engineering, Yale School of Medicine, P.O. Box 9812, New Haven, CT 06536-9812.

are propagated by chemokines such as CCL2, previously known as monocyte chemoattractant protein MCP-1.<sup>10</sup> CCL2 belongs to a small family of CC-type chemokines that can be synthesized by almost every cell type. Its specificity is limited to the distribution of its sole receptor, CCR2, which is restricted mainly to monocytes/macrophages, memory T lymphocytes, and natural killer cells. Binding of CCL2 to CCR2 triggers a number of responses including intracellular calcium mobilization, cytoskeletal rearrangement, and activation of MAP kinase, and CCL2 has been shown to be critical for the migratory responses of monocytes both *in vitro* and *in vivo*.<sup>10,11</sup> In addition, CCR2-null mice are deficient in recruiting monocytes to sites of inflammation in several models, suggesting that the CCL2-CCR2 interaction is critical for this process and cannot be compensated by another CCL-CCR interaction.<sup>12</sup> Evidence for a possible dual role of CCL2 can be found in studies of CCL2-null mice. These mice display a significant reduction in monocyte infiltration following IP injection of thioglycollate,<sup>13</sup> but have a normal macrophage content in cutaneous wounds.<sup>14</sup> In the latter model, CCL2-null mice display a delayed healing response, characterized by delayed wound closure that appears to be associated with reduced neovascularization. This observation prompted the investigators to conclude that CCL2 was not essential for monocyte recruitment to wound sites, but that it played a role in proper monocyte/macrophage function.

We asked whether CCL2 was critical for the recruitment of monocytes to sites of biomaterial implantation. Previously, CCL2 was shown to be expressed on monocytes recruited to biomaterial implantation sites at early time points, ie, day 2.<sup>15</sup> We have also found CCL2 to be present on FBGC at 2 and 4 weeks following implantation, suggesting that it can influence the activities of monocytes, macrophages, and FBGC throughout the progression of the FBR. More importantly, implantation studies in CCL2-null mice demonstrated a requirement for this chemokine in the formation of FBGC, but not in the recruitment and migration of macrophages. These findings were supported by studies of monocyte fusion *in vitro*.

## Materials and Methods

### Materials

Rat anti-mouse Mac 3 Ab was obtained from BD Pharmingen (San Diego, CA), rat anti-mouse F4/80 Ab from Serotec (Raleigh, NC), anti-mouse MCP-1/CCL2 from Santa Cruz Biotech (Santa Cruz, CA), and anti-human CCL2/MCP-1, clone 24822.111 from R&D Systems (Minneapolis, MN). A Vectastain ABC kit for immunohistochemistry was purchased from Vector Laboratories (Burlingame, CA). A *Limulus* amoebocyte endotoxin assay was purchased from Associates of Cape Cod Inc. (East Falmouth, MA, USA). ECL Western detection was purchased from Amersham (Piscataway, NJ) and a bicinchoninic acid (BCA) protein detection kit from Bio-Rad (Hercules, CA). Polyvinyl alcohol (PVA) sponges (Clinicel, Grade 3) were purchased from M-PACT (Eudora, KS, USA). Filters

(0.45- $\mu$ m pore size, mixed cellulose ester) were purchased from Millipore. TGF- $\beta_1$  ELISA kits and human recombinant IL-4 were purchased from R&D systems, and GM-CSF was a kind gift from Immunex (Seattle, WA). Soluble collagen (Vitrogen) was purchased from Cohesive Sciences (Palo Alto, CA).

### Preparation of Biomaterials

Twenty-five-mm<sup>2</sup> Millipore filters and 6-mm-diameter sponges were soaked in 95% ethanol for 24 hours, rinsed extensively with phosphate-buffered saline (PBS), and stored in endotoxin-free PBS until implantation. Biodegradable alginate (5%)-based scaffolds with pore size of 20  $\mu$ m (Kyriakides TR, Nair PD, Mezmarich NAK, Bornstein P, Donaldson E, Hauch KD, Nerem RD, Ratner BD, manuscript in preparation) were prepared and gas-sterilized in ethylene oxide. Some scaffolds were placed in endotoxin-free PBS for analysis. The endotoxin content of the PBS storage solution, for filters, sponges, and scaffolds, was determined with the *Limulus* amoebocyte endotoxin assay according to the supplier's instructions. Endotoxin concentration was found to be below 2 endotoxin units (EU)/ml in all samples.

### Preparation of Gene-Activated Matrix-Coated Biomaterials

pMT-7ND is a mammalian expression vector containing DNA-encoding human MCP-1 lacking amino acids 2–8 and a FLAG tag, driven by the SV40 promoter. This construct was included in a gene-activated matrix (GAM) on filters, as described previously.<sup>16</sup> Filters were sterilized by overnight incubation in 95% ethanol, followed by two 12-hour washes in endotoxin-free sterile water. Sterilized biomaterials were immersed in a collagen/pMT-7ND or a collagen/pcDNA3 (DNA control) solution for 30 minutes at 4°C with continuous rotation. All biomaterials were then frozen ( $-70^{\circ}\text{C}$ ) for 15 minutes and lyophilized. For preparation of the collagen/plasmid GAM, soluble collagen was neutralized by addition of Dulbecco's Minimal Essential Media (DMEM) and endotoxin-free 0.1 mol/L NaOH, and then mixed with the plasmid DNA (1.5 mg collagen/mg DNA). All GAM preparations were analyzed for endotoxin content, as described above, and found to contain less than 1 EU/ml.

### Implantation of Biomaterials

All procedures were performed in accordance with the regulations adopted by the National Institutes of Health and approved by the Animal Care and Use Committee of the University of Washington. S.C. implantations were performed essentially as described previously.<sup>17,18</sup> A total of 16 CCL2-null and 24 control mice were used for implantations. Each mouse received two implants, providing for eight implants per group, per material, per time point. The genetic background of CCL2-null mice is 93% C57BL/6 and 7% SJL, and of control mice, C57BL/6.

Previous examination of the FBR in wild-type mice of several genetic backgrounds, ie, 129SvJ, C57BL6, mixed 129SvJ/C57BL6 has shown it to be essentially identical (unpublished observations). Mice were sex- and age-matched (3 to 4 months of age). Implants were excised *en bloc*, at 2 or 4 weeks following implantation, as described previously.<sup>18</sup> For the *in vivo* blockade of CCL2, eight mice were used, each receiving a pMT-7ND GAM-coated filter and a control GAM-coated filter.

### Preparation and Analysis of Sponge Fluid

PVA sponges were excised 14 days following implantation and dissected cleanly of surrounding tissue. Sponge fluid was recovered by centrifugation as described previously.<sup>18</sup> The protein content of fluids was determined by the BCA method and equal amounts of protein per sample were analyzed by ELISA, as described previously.<sup>19</sup>

### Histology and Immunohistochemistry

Explanted biomaterials were excised and fixed in 10% zinc-buffered formalin for 24 hours. Following processing and embedding, 6- $\mu\text{m}$  sections (eight per sample) were stained with hematoxylin and eosin (H&E) and Masson's trichrome. Capsule thickness was measured at 10 different locations (five per side) with the aid of an ocular micrometer. Immunolocalization of Mac3 (1:500), F4/80 (1:3000), and CCL2 (1:400) was performed according to the supplier's instructions. All secondary peroxidase-conjugated Ab were used at 1:200 dilution. Controls included sections treated with pre-immune sera. Sections from CCL2-null mice served as a negative control for the immunodetection of CCL2. The number of FBGC was estimated from H&E- and Mac3-stained sections (eight per sample). The number of nuclei per FBGC was estimated from the analysis of over 200 cells for control and over 100 cells for CCL2-null mice.

### Monocyte Isolation and *In Vitro* Fusion

Blood was collected from healthy volunteers (200 ml per volunteer) who had not taken any anti-inflammatory drugs for at least 24 hours, according to University of Washington guidelines. Monocytes were isolated and induced to fuse as described previously.<sup>20</sup> Briefly,  $1 \times 10^6$  leukocytes were added to each well of 24-well plates (nontissue culture-treated polystyrene) in 1 ml of RPMI culture medium, supplemented with 25% autologous serum, and allowed to attach for 2 hours at 37°C, 5% CO<sub>2</sub>. Non-adherent cells were removed by washing to leave only monocytes. To induce fusion, media containing 25% autologous serum (heat-treated at 56°C for 1 hour), GM-CSF (10 ng/ml), and IL-4 (10 ng/ml) were added on days 3 and 7. Under these conditions, within 10 days approximately 60 to 70% of the cells became part of multinucleated cells (containing three or more nuclei). Selected wells received 200 ng/ml of MCP-1 (9–76) peptide, an inactive control peptide MCP-1 (9–76-4A), 5  $\mu\text{g}$  anti-human MCP-1/CCL2 function-blocking Ab, or 5  $\mu\text{g}$  iso-

type control Ab. The peptide MCP-1 (9–76-4A) contains four alanines in place of four cysteines. On day 10, cells were fixed with methanol and monocyte fusion was assessed by analyzing May-Grünwald/Giemsa-stained cells.<sup>21</sup> In addition, the number of nuclei per giant cell was determined. For each condition, a total of three wells were analyzed and each experiment was repeated twice.

## Results

### Effect of CCL2 Deficiency on Biomaterial Encapsulation, Sponge Granuloma, and FBGC Formation

Implantation of filters and sponges in CCL2-null mice did not elicit any adverse reactions. Overall, the mice tolerated the implants as well as their wild-type counterparts, and all mice survived the surgical procedure and implantation period. Examination of sections from filters stained with H&E revealed that the formation of FBGC was reduced in CCL2-null mice (Figure 1, B and D). Specifically, we observed a 75% reduction in the number of FBGC surrounding filters and a 90% reduction in the number of FBGC within sponges implanted in CCL2-null mice (Figure 1E). The difference in FBGC formation between the two implants may be due to the different implantation periods, 2 weeks for sponges and 4 weeks for filters. We examined sponges at the 2-week time point because at this time porous biomaterials are not fully encapsulated. Alternatively, the differences may be due to the unique properties of the two materials, including the increased surface area of the porous sponge. Analysis of longer-term, 2-month implants showed FBGC formation and encapsulation similar to 4-week implants (data not shown), suggesting that the increased implantation time was not associated with an additional reduction in the number of FBGC. To exclude the possibility that the reduction of FBGC formation in CCL2-null mice was due to a greater number of cells fusing to form one FBGC, we determined the number of nuclei per giant cell. We found that this number was significantly reduced rather than increased in CCL2-null FBGC (Figure 1F).

### Lack of Effect of FBGC Depletion on Encapsulation

Despite the reduced formation of FBGC in the CCL2-null mice, the encapsulation of filter implants was not compromised. Masson's trichrome stain revealed that the deposition of collagen in the capsule proceeded normally between 2 and 4 weeks. At 4 weeks, capsule thickness was equivalent between CCL2-null ( $77 \pm 50 \mu\text{m}$ ) and control mice ( $63 \pm 25 \mu\text{m}$ ). Similar observations have been made by analysis of polyvinyl alcohol sponges. Specifically, encapsulation ( $172 \pm 78$  versus  $158 \pm 43 \mu\text{m}$ ) and invasion ( $162 \pm 29$  versus  $151 \pm 44 \mu\text{m}$ ) of sponges did not differ between CCL2-null and control mice. Because FBGC have been shown to secrete pro-

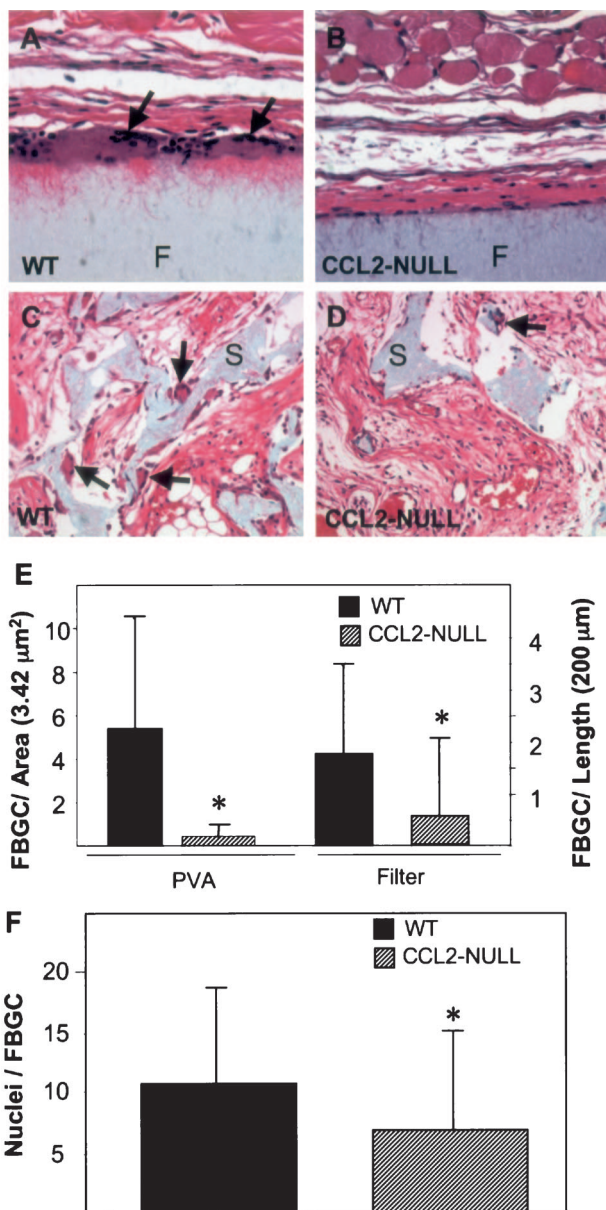


**Figure 1.** CCL2-null mice display reduced FBGC formation. Sponges and filters were implanted s.c. in mice for a period of 2 and 4 weeks, respectively. Representative images are shown of sections stained with H&E from filters (F), (A and B) and sponges (S), (C and D), implanted in wild-type (A and C) and CCL2-null mice (B and D). Arrows indicate the presence of FBGC. Magnification,  $\times 400$  (A and B),  $\times 200$  (C and D). **E:** The number of FBGC (cells with three or more nuclei) per high-power field was estimated by examination of H&E- and Mac-3-stained sections ( $n = 50$ ). The number of FBGC per unit length surrounding filters was also estimated because capsules did not occupy an entire high-power microscopic field (see A and B). **(F)** Reduced number of nuclei in CCL2-null FBGC. The number of nuclei per FBGC (from sponges and filters) was determined by microscopic examination of over 100 FBGC per genotype. The location of nuclei within FBGC was similar between the two groups. The data represent mean  $\pm$  SEM. \*,  $n = 8$ ; statistical significance,  $P \leq 0.05$ , when compared with wild-type using Student's *t*-test.

fibrotic TGF- $\beta_1$ ,<sup>22</sup> we examined the levels of this growth factor in sponges implanted for 2 weeks. Analysis of sponge fluids by ELISA indicated that the level of TGF- $\beta_1$  in CCL2-null samples ( $225 \pm 11$  pg/ml) was similar to control levels ( $214 \pm 27$  pg/ml).

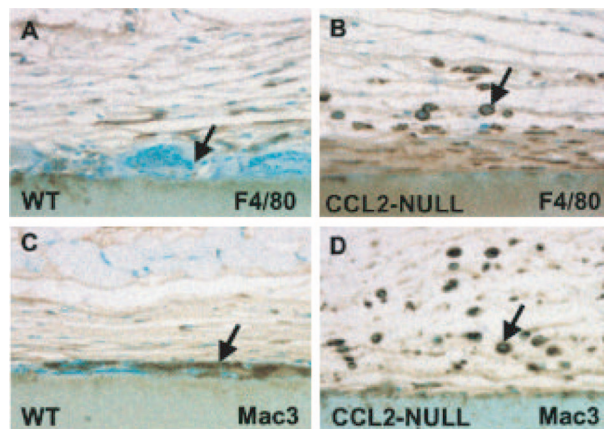


**Figure 2.** Increased presence of cells of the monocyte lineage in CCL2-null capsules. Representative sections of capsules, implanted s.c. for 4 weeks and stained with anti-F4/80 (A and B) and anti-Mac3 (C and D) Ab from wild-type (A and C) and CCL2-null (B and D) mice are shown. Ab stains were visualized with the peroxidase reaction (brown color). Arrows indicate the presence of FBGC (A and C) and macrophages (B and D). FBGC are not immunoreactive with F4/80 (A) but can be detected with Mac3 (C). The abundance of mononuclear macrophages in CCL2-null sections is evident. Nuclei are visualized with methyl green counterstain. Original magnification,  $\times 400$ .

### Lack of an Effect of CCL2 Deficiency on Monocyte Recruitment

To distinguish between reduced monocyte recruitment and reduced macrophage fusion as an explanation for the reduced FBGC formation, we performed an immunohistological analysis of sections with two Ab specific for surface receptors of cells of the monocyte-FBGC lineage. First, we used anti-F4/80 Ab that recognizes a 160-kd surface glycoprotein expressed by most murine macrophages. Second, we used anti-Mac3 Ab that recognizes a 110-kd surface glycoprotein whose expression increases during the differentiation of monocytes to activated macrophages. As shown in Figure 2, both Ab showed the presence of abundant macrophages in CCL2-null mice (B and D). On the contrary, FBGC immunoreactive for Mac3 were absent (D). In wild-type mice the presence of F4/80-positive macrophages was reduced (A) whereas the presence of Mac3-positive FBGC was prominent (C). Immunohistochemical analysis of sections with the anti-macrophage Ab, BM-8, produced results identical to those obtained with the F4/80 Ab (data not shown). To quantify macrophages we analyzed sections from PVA sponges because we could obtain entire high-power fields for analysis. We were unable to do so from capsules surrounding filters. CCL2-null mice had slightly more F4/80-positive cells ( $84.5 \pm 38.3$ ) and Mac3-positive cells ( $55.8 \pm 24.4$ ) than wild-type mice ( $51.4 \pm 28.4$  for F4/80;  $52.3 \pm 32.1$  for Mac-3). However, none of the differences was significant ( $p > 0.5$ ). These observations indicate that the recruitment of monocytes to the implant site is not compromised in CCL2-null mice.

### Effect of CCL2 Deficiency on Biomaterial Degradation

To examine whether biomaterials sustain reduced damage in CCL2-null mice as a result of reduced numbers of

FBGC, we implanted a hydrolysis-resistant, biodegradable, alginate-based scaffold and examined the FBR 4 weeks following implantation. Scaffolds in CCL2-null mice were invaded predominantly by mononuclear inflammatory cells, failed to induce FBGC formation, and lacked fibrovascular invasion (Figure 3A). In contrast, scaffolds implanted in wild-type mice displayed significant FBGC and blood vessel formation, and deposition of mature extracellular matrix (Figure 3B). Scaffolds in CCL2-null mice were also subjected to reduced damage, as approximately 50% more of the scaffold remained intact in these mice in comparison to wild-type (Figure 3C).

### FBGC Cells Are Immunoreactive for CCL2

The inferred participation of CCL2 in fusion prompted us to investigate its presence in FBGC. By using a commercially available anti-CCL2 Ab, we were able to detect CCL2 in macrophages and on the surface of FBGC surrounding filters and sponges implanted s.c. in control mice (Figure 4, A and B). No immunoreactivity could be detected in the rare FBGC in CCL2-null mice (Figure 4C) or in wild-type mice stained with an isotype control Ab (Figure 4D).

### Effect of Blockade of CCL2 in Vivo on FBGC Formation

To limit FBGC formation *in vivo* we used an established method for localized gene delivery.<sup>23</sup> Specifically, GAM-coated filters were implanted s.c. in wild-type mice. Administration of DNA containing a shortened version of CCL2 (pMT-7ND), lacking seven amino acids from the amino terminus, has previously been shown to block the activity of endogenous CCL2.<sup>24,25</sup> After a 4-week implantation period, filters coated with a pMT-7ND GAM elicited an FBR that was similar to that of MCP-1-null mice in regard to encapsulation, macrophage content, and FBGC formation (Figure 5, B and D; see Figures 1 and 2). Control GAM (vector DNA)-coated filters elicited macrophage recruitment and induced FBGC formation in a manner similar to that in wild-type mice (Figure 5, C and D). FBGC formation around pMT-7ND-coated filters was reduced by over 50%, whereas control filters induced normal FBGC formation (Figure 5D). Furthermore, FBGC on the surface of pMT-7ND GAM-coated filters were small, and contained a limited number of nuclei (see arrowheads in Figure 5A) in comparison to FBGC on DNA control-treated filters (see arrowhead in Figure 5C) and untreated filters (see arrows in Figure 1A). To confirm the expression of plasmid genes, we stained sections with an anti-FLAG FITC-conjugated Ab. FLAG expression was detected in cells surrounding pMT-7ND-treated filters (see arrows in Figure 5F), but not pcNDA3-treated filters (Figure 5E).

### Effect of CCL2 Inhibition on Monocyte Fusion

Human monocytes can be induced to form multinucleated giant cells by fusion following the addition of IL-4

and GM-CSF to the culture medium. In this *in vitro* system, addition of a CCL2-inhibitory peptide (MCP1 9–76), but not an inactive control peptide (MCP1 9–76-4A), resulted in a significant reduction in fusion (Figure 6). The utility of MCP1 9–76 in blocking the activity of CCL2 has been demonstrated both *in vitro*<sup>26,27</sup> and *in vivo*.<sup>28</sup> The prominent appearance of fused cells (Figure 6A) was not observed in MCP1 9–76-treated wells (Figure 6B). Overall, both the number of nuclei (Figure 6C) and percentage fusion (Figure 6D) were reduced in the MCP1 9–76 treatment group. In contrast, the addition of the control peptide did not influence these two parameters. Addition of the peptides did not appear to influence cell survival negatively, since the cell number per well at the end of the treatments ( $2193 \pm 165$  for MCP1 9–76 and  $2373 \pm 177$  for MCP1 9–76-4A) were similar to those of controls ( $2436 \pm 243$ ) ( $n = 5$ ,  $P > 0.1$ ). In addition, MCP1 9–76-treated cells displayed normal morphology (Figure 6B).

Similar results were obtained by the addition of an anti-human MCP1/CCL2 Ab (Figure 7). However, the reduction in fusion following the addition of Ab (65%) was more pronounced than the addition of MCP1 9–76 peptide (50%). Addition of an isotype control Ab did not have an effect on fusion.

### Discussion

FBGC formation, a hallmark of the FBR, is harmful to implanted biomaterials because it contributes to the degradation of the biomaterial surface, and leads to “stress cracking”, tissue fibrosis, and a chronic inflammatory response.<sup>8</sup> FBGC are thought to be a source of chemokines that mediate the recruitment of neutrophils and lymphocytes.<sup>8,15</sup> The latter, by interacting with adherent macrophages and FBGC, cause an increase in the local concentration of cytokines and growth factors, and modulate the function of surrounding cells, such as fibroblasts, that are primarily responsible for the deposition of the collagenous matrix within the capsule. FBGC have also been shown to secrete pro-fibrotic latent transforming growth factor- $\beta_1$  during the late chronic inflammatory response in an *in vivo* experimental model.<sup>22</sup> Thus, inhibition or limitation of FBGC formation is expected to enhance biocompatibility by limiting biomaterial-induced inflammation and subsequent undesirable events.

Because FBGC are formed by the fusion of macrophages at the implant site, we hypothesized that CCL2, a chemotactic mediator for monocytes, might play a critical role in the FBR. In the present study we report that CCL2 is not required for monocyte recruitment and the development of the FBR when biomaterials are implanted in the subcutaneous space. The presence of numerous macrophages within the foreign body capsules and sponge granulomas, formed s.c. in CCL2-null mice, is surprising but consistent with the observations of Low et al<sup>14</sup> during the healing of cutaneous wounds in these mice. Thus, despite the well-documented inability of CCL2-null mice to recruit monocytes in models of inflammation, such as acute peritonitis, they appear to be able recruit monocytes to the subcutaneous space. Consis-

tent with these observations, preliminary studies in our laboratory have demonstrated reduced monocyte recruitment following implantation of biomaterials in the peritoneal cavity of CCL2-null mice (Kyriakides TR, Rollins BJ, Bornstein P, unpublished observation). The biological ex-

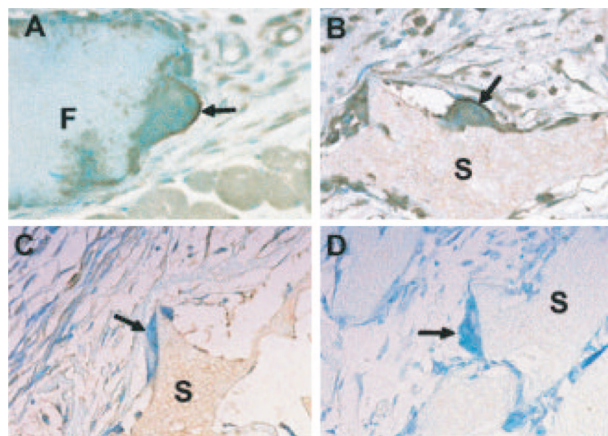
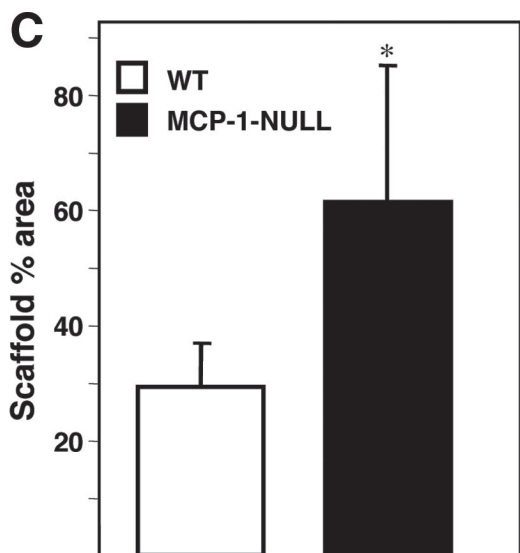
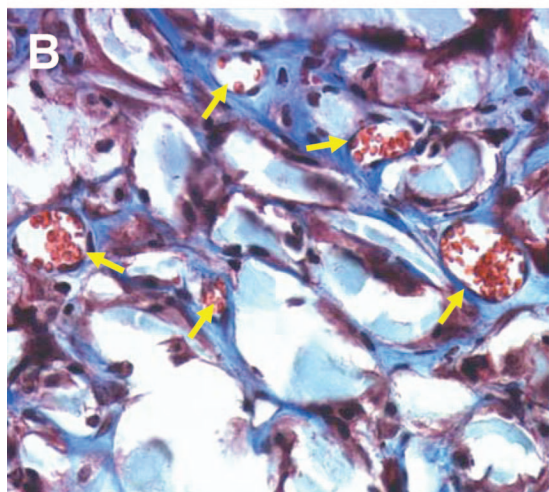
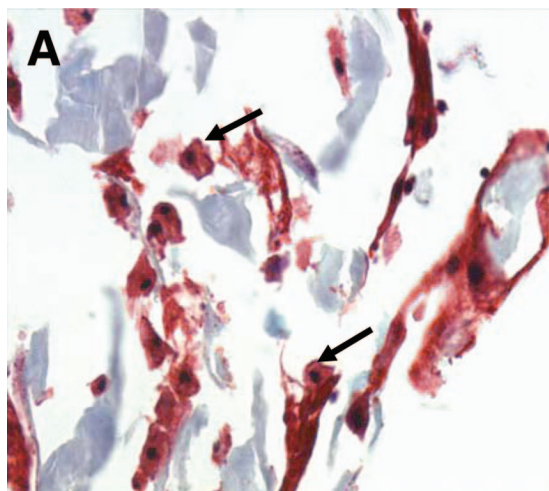


**Figure 4.** CCL2 is present in FBGC. Sections of a filter (A) and sponges (B–D) implanted s.c. in wild-type mice for 4 and 2 weeks, respectively, were stained with anti-CCL2 Ab (A–C) or control Ab (D) and visualized with the peroxidase reaction (brown color). Arrows indicate the presence of FBGC in wild-type mice (A–B, D) and CCL2-null mice (C). F and S denote areas occupied by filter and sponge, respectively. The FBGC in A and B are positive for CCL2, whereas those in C and D are negative. Nuclei are visualized with methyl green counterstain. Original magnification,  $\times 400$ .

planation for this distinction in CCL2-null mice is unclear. Perhaps monocyte recruitment into the peritoneal cavity depends solely on CCL2, whereas other chemokines can perform the same function in the subcutaneous space. In addition, the recruitment of monocytes and the activation of macrophages may depend on the function of resident macrophages. It is possible that the resident macrophage population in skin differs functionally from that in the peritoneum. Differences in macrophage function based on the tissue distribution have been described.<sup>29,30</sup>

CCL2 appears to have multiple roles in macrophage function, including one in post-recruitment events. Our results in CCL2-null mice indicate that it is required for macrophage fusion. To verify this requirement we inhibited the function of CCL2 in wild-type mice during the FBR. Since the biological effects of CCL2 are mediated by binding to the chemokine receptor CCR2, found primarily on monocytes, we designed an experiment to target this interaction. Several investigators have shown that the NH<sub>2</sub>-terminus of CCL2 is required for biological activity. Thus, recombinant and synthetic versions of CCL2 that lack amino acids from the NH<sub>2</sub>-terminus are deficient in eliciting monocyte chemotaxis.<sup>31,32</sup> In this study we show that the localized expression of an NH<sub>2</sub>-

**Figure 3.** Reduced biomaterial degradation in CCL2-null mice. Representative sections are shown of scaffold implanted s.c. for 4 weeks in CCL2-null (A) and wild-type (B) mice and stained with Masson's trichrome. In CCL2-null mice, scaffolds underwent minimal degradation and collagen deposition. The majority of the cells present within the scaffold were mononuclear inflammatory cells (arrows), and the scaffold was not subjected to fibrovascular invasion. In wild-type mice (B), scaffolds were invaded by a fibrovascular response, evident by the presence of collagen (bright blue color) and blood vessels (yellow arrows). In addition, numerous FBGC were observed. Scaffold remnants have a grayish blue color appearance. Images were taken from the center area of the scaffolds. Original magnification,  $\times 200$ . C: The average percentage of a high-power field (0.04  $\mu\text{m}^2$ ) occupied by scaffold 4 weeks following implantation was estimated with the aid of imaging software. A total of three scaffolds per genotype were used to obtain images and a total of 24 images per scaffold were analyzed. The data represent mean  $\pm$  SEM. \*, Statistical significance,  $P \leq 0.05$ , when compared with wild-type using Student's *t*-test.

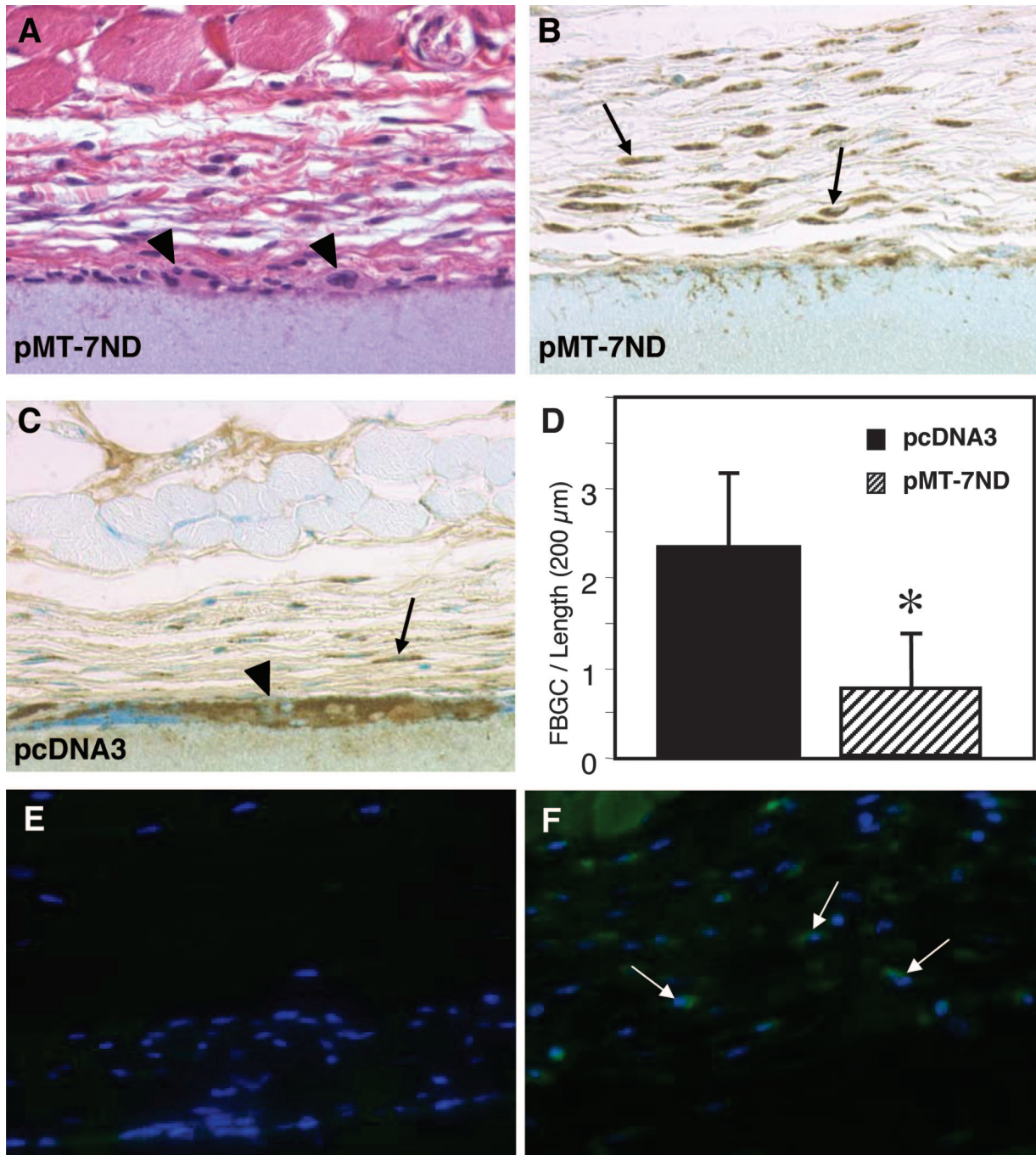


**Figure 5.** Reduced FBGC formation *in vivo* by localized blockade of CCL2. Representative sections are shown of pMT-7ND GAM- (A and B) and pcDNA3 GAM- (C) coated filters implanted s.c. for 4 weeks in wild-type mice and stained with H&E (A) or the macrophage marker Mac3 and visualized with the peroxidase reaction (B and C). In A–C, arrows indicate individual macrophages, and arrowheads indicate FBGC. Magnification,  $\times 400$  (A–C). (D) The number of FBGC (cells with three or more nuclei) per unit length of filter was estimated by the examination of Mac3-stained sections. The data represent mean  $\pm$  SEM,  $n = 75$ ; \*, statistical significance,  $P \leq 0.05$ . Representative sections are shown of pMT-7ND GAM- (E) and pcDNA3 GAM- (F) coated filters stained with an anti-FLAG FITC-conjugated Ab. Arrows in F indicate FLAG-expressing cells in the capsule. Magnification,  $\times 200$  (E–F).

terminally truncated CCL2 during the foreign body response in wild-type mice resulted in reduced FBGC formation without a concomitant decrease in macrophage recruitment. Furthermore, qualitative analysis of the limited number of FBGC that formed in the presence of pMT-7ND revealed that they were smaller in size and involved a limited number of nuclei. Therefore, we conclude that CCL2 is required for normal macrophage fu-

sion. Because reagents that can distinguish between truncated and endogenous CCL2 are not available, we examined the duration of pMT-7ND expression by the immunolocalization of a FLAG tag, and found it to be present. This observation is consistent with a previous study, in the same *in vivo* setting, where we reported expression of other exogenous genes for at least 4 weeks.<sup>16</sup>

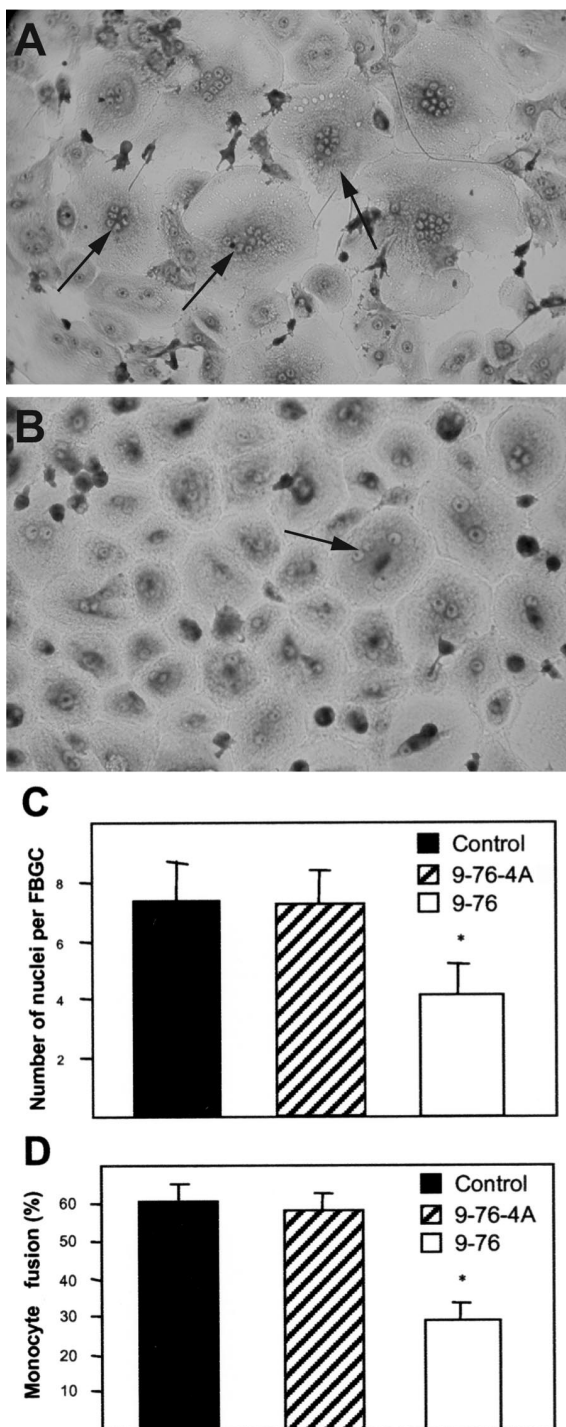


**Figure 6.** Reduced fusion following treatment of monocytes with a CCL2 inhibitory peptide. Monocytes were induced to fuse in the presence of an inactive, control peptide MCP-1 (9-76-4A) (A) or active, inhibitory peptide MCP-1 (9-76) (B). A total of 10 fields per well and five wells per group were analyzed. Cells with three or more nuclei were classified as FBGC (examples denoted by arrows in A and B). Magnification,  $\times 200$ . The average number of nuclei per giant cell is shown (C). Percentage fusion was determined by estimating the number of nuclei in FBGC in relation to the total number of nuclei (D). The data represent mean  $\pm$  SEM. \*, Statistical significance,  $P \leq 0.05$ , when compared with control peptide treatment using Student's *t*-test.

The existence of a role for CCL2 in macrophage fusion is also supported by experiments *in vitro* with human peripheral blood monocytes that are favored by investi-

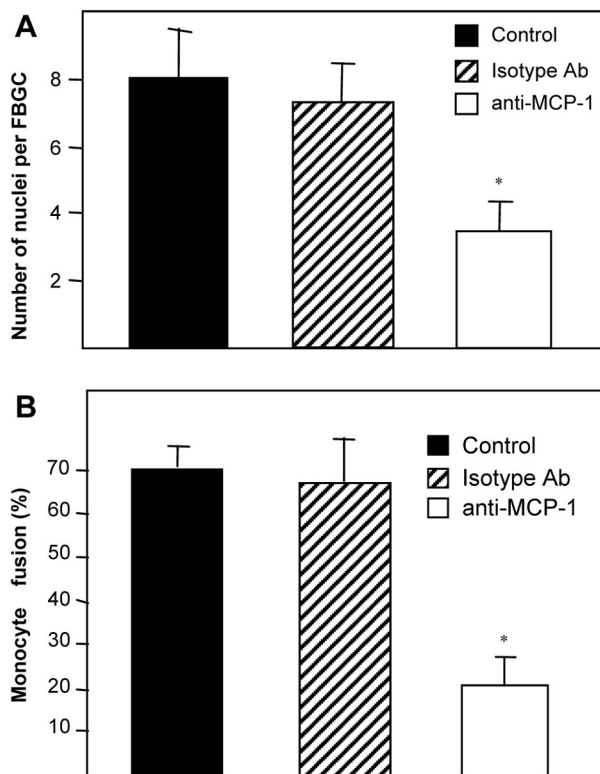


**Figure 7.** Reduced fusion following treatment of monocytes with a function-blocking anti-MCP-1 Ab. Monocytes were treated as described in the text and a total of 10 fields per well and five wells per group were analyzed. Cells with three or more nuclei were classified as FBGC (A). Percentage fusion was determined by estimating the number of nuclei in FBGC in relation to the total number of nuclei (B). The data represent mean  $\pm$  SEM. \*, Statistical significance,  $P \leq 0.05$ , when compared with isotype control IgG treatment using Student's *t*-test.

gators who study FBGC formation. This model takes advantage of the isolation of a large number of monocytes that can be induced to fuse in a manner and time frame that mirrors FBGC formation *in vivo*. Previous studies using this *in vitro* system have identified fusion-related monocyte surface proteins, such as the receptors for mannose and  $\beta_1$  integrin,<sup>21,33</sup> and in our studies addition of a CCL2-blocking peptide or Ab in this model caused a significant reduction in macrophage fusion. Specifically, both overall fusion and the number of nuclei per FBGC were decreased, without a concomitant decrease in the number of cells. Thus, the reduction of FBGC formation in CCL2-null mice can be attributed directly to the deficiency in CCL2.

A fusion receptor, SHPS-1, has been identified in a different *in vitro* fusion system that utilizes alveolar macrophages.<sup>34</sup> We were also able to detect this receptor on FBGC *in vivo* (not shown). Recently, it has been suggested that SHPS-1 might act as a negative regulator in the phagocytosis of platelets by macrophages.<sup>35</sup> It is intriguing to speculate that induction of SHPS-1 expression is associated with frustrated phagocytosis, a term coined to explain the propensity of macrophages to fuse when they encounter large foreign objects. The expression of a number of other surface-associated molecules might also be altered. For example, it was recently shown



that CD47/integrin-associated protein is a ligand for SHPS-1, and that their interaction is critical for fusion *in vitro*.<sup>36,37</sup> Furthermore, the participation of CD44, an integral membrane glycoprotein, in alveolar macrophage fusion has been documented.<sup>38</sup> The presence of CD44 on FBGC *in vivo* has also been demonstrated.<sup>39</sup> However, its role, if any, in FBGC formation *in vivo* has not been defined.

The reduction of FBGC formation in CCL2-null mice provides us with a unique opportunity to study the role of these cells in the FBR. To our knowledge, experiments describing a nearly complete inhibition of FBGC formation have not been reported. van Luyn et al<sup>40</sup> examined the role of rat macrophages in the degradation of implanted sheep dermal collagen following chemical depletion of these cells. The results of this study showed that degradation was delayed and FBGC formation was somewhat reduced. However, an examination of the contribution of FBGC to the FBR was not pursued. Iizuka et al<sup>41</sup> showed that colony-stimulating factor-1-deficient mice form smaller FBGC with a reduced number of nuclei in a subcutaneous implant model. No differences in the fibrotic response were reported.

Numerous reports indicate that encapsulation is influenced by several factors, including site of implantation, wettability properties of the biomaterial, biomaterial porosity, and surface texture (reviewed in<sup>2</sup>). More recently, Brodbeck et al<sup>42</sup> showed that hydrophilic and anionic substrates increase macrophage apoptosis in the *in vivo* rat cage implant model. No effects on additional parameters of the FBR were examined. Our results show that FBGC are not critical for progression of the encapsulation process. Rather, they indicate that macrophages may be the key cell type in the development of the FBR and, especially, fibrosis. We have found that the levels of TGF- $\beta_1$  are not altered as a result of the reduction in FBGC formation. Thus, it is possible that macrophages can provide pro-fibrotic signals to fibroblasts. This suggestion is supported by our observation of the events following intraperitoneal (i.p.) implantation of filters, where compromised macrophage recruitment was associated with the lack of a fibrotic response (Kyriakides TR, Rollins BJ, Bornstein P, unpublished observation).

The present study leads us to the conclusion that the FBR is a host-driven response that can be altered by the modulation of key molecular players. For example, we have previously shown that neovascularization of the foreign body capsule can be increased following the inhibition of the potent matricellular angiogenesis inhibitor, thrombospondin-2.<sup>16</sup> Here we have expanded our studies to the analysis of the FBR in CCL2-null mice, a mouse model with a previously described deficient inflammatory response. We have described the existence of a previously unknown role for CCL2 in macrophage fusion, and demonstrated that FBGC formation is not essential for encapsulation. In addition, our results support a proposed role for FBGC in the causation of surface damage as evidenced by the alterations in biomaterials in these mice. Thus, strategies to limit FBGC formation, in addition to preventing surface damage, may provide for biological control of the degradation rate of biodegradable biomaterials.

Detailed investigation of this model should lead to the development of strategies that can improve the performance and longevity of implanted biomaterials.

### Acknowledgments

We thank Greg Priestley and Emily Stainbrook for technical assistance with animal husbandry, and Azin Agah for assistance with immunohistochemistry and ELISA.

### References

1. Tang L, Eaton JW: Natural responses to unnatural materials: a molecular mechanism for foreign body reactions. *Mol Med* 1999, 5:351–358
2. Mikos AG, McIntire LV, Anderson JM, Babensee JE: Host response to tissue engineered devices. *Adv Drug Deliv Rev* 1998, 33:111–139
3. Tang L, Eaton JW: Inflammatory responses to biomaterials. *Am J Clin Pathol* 1995, 103:466–471
4. Woodward SC: How fibroblasts and giant cells encapsulate implants: considerations in design of glucose sensors. *Diabetes Care* 1982, 5:278–281
5. Ratner BD: New ideas in biomaterials science: a path to engineered biomaterials. *J Biomed Mater Res* 1993, 27:837–850
6. Ratner BD: The engineering of biomaterials exhibiting recognition and specificity. *J Mol Recognit* 1996, 9:617–625
7. Singer AJ, Clark RA: Cutaneous wound healing. *N Engl J Med* 1999, 341:738–746
8. Anderson JM: Multinucleated giant cells. *Curr Opin Hematol* 2000, 7:40–47
9. Zhao Q, Topham N, Anderson JM, Hiltner A, Lodoen G, Payet CR: Foreign-body giant cells and polyurethane biostability: *in vivo* correlation of cell adhesion and surface cracking. *J Biomed Mater Res* 1991, 25:177–183
10. Gu L, Tseng SC, Rollins BJ: Monocyte chemoattractant protein-1. *Chem Immunol* 1999, 72:7–29
11. Newton RC, Vaddi K: Biological responses to C-C chemokines. *Methods Enzymol* 1997, 287:174–186
12. Kuziel WA, Morgan SJ, Dawson TC, Griffin S, Smithies O, Ley K, Maeda N: Severe reduction in leukocyte adhesion and monocyte extravasation in mice deficient in CC chemokine receptor 2. *Proc Natl Acad Sci USA* 1997, 94:12053–12058
13. Lu B, Rutledge BJ, Gu L, Fiorillo J, Lukacs NW, Kunkel SL, North R, Gerard C, Rollins BJ: Abnormalities in monocyte recruitment and cytokine expression in monocyte chemoattractant protein 1-deficient mice. *J Exp Med* 1998, 187:601–608
14. Low QE, Drugea IA, Duffner LA, Quinn DG, Cook DN, Rollins BJ, Kovacs EJ, DiPietro LA: Wound healing in MIP-1 $\alpha$ ( $-/-$ ) and MCP-1( $-/-$ ) mice. *Am J Pathol* 2001, 159:457–463
15. Rhodes NP, Hunt JA, Williams DF: Macrophage subpopulation differentiation by stimulation with biomaterials. *J Biomed Mater Res* 1997, 37:481–488
16. Kyriakides TR, Hartzel T, Huynh G, Bornstein P: Regulation of angiogenesis and matrix remodeling by localized, matrix-mediated anti-sense gene delivery. *Mol Ther* 2001, 3:842–849
17. Kyriakides TR, Leach KJ, Hoffman AS, Ratner BD, Bornstein P: Mice that lack the angiogenesis inhibitor, thrombospondin 2, mount an altered foreign body reaction characterized by increased vascularity. *Proc Natl Acad Sci USA* 1999, 96:4449–4454
18. Kyriakides TR, Zhu YH, Yang Z, Huynh G, Bornstein P: Altered extracellular matrix remodeling and angiogenesis in sponge granulomas of thrombospondin 2-null mice. *Am J Pathol* 2001, 159:1255–1262
19. Agah A, Kyriakides TR, Lawler J, Bornstein P: The lack of thrombospondin-1 (TSP1) dictates the course of wound healing in double-TSP1/TSP2-null mice. *Am J Pathol* 2002, 161:831–839
20. McNally AK, Anderson JM: Interleukin-4 induces foreign body giant cells from human monocytes/macrophages: differential lymphokine regulation of macrophage fusion leads to morphological variants of multinucleated giant cells. *Am J Pathol* 1995, 147:1487–1499
21. McNally AK, Anderson JM: Beta1 and beta2 integrins mediate adhe-

- sion during macrophage fusion and multinucleated foreign body giant cell formation. *Am J Pathol* 2002, 160:621–630
22. Hernandez-Pando R, Bornstein QL, Aguilar Leon D, Orozco EH, Madrigal VK, Martinez Cordero E: Inflammatory cytokine production by immunological and foreign body multinucleated giant cells. *Immunology* 2000, 100:352–358
  23. Bonadio J: Tissue engineering via local gene delivery. *J Mol Med* 2000, 78:303–311
  24. Egashira K, Koyanagi M, Kitamoto S, Ni W, Kataoka C, Morishita R, Kaneda Y, Akiyama C, Nishida KI, Sueishi K, Takeshita A: Anti-monocyte chemoattractant protein-1 gene therapy inhibits vascular remodeling in rats: blockade of MCP-1 activity after intramuscular transfer of a mutant gene inhibits vascular remodeling induced by chronic blockade of NO synthesis. *FASEB J* 2000, 14:1974–1978
  25. Egashira K, Zhao Q, Kataoka C, Ohtani K, Usui M, Charo IF, Nishida K, Inoue S, Katoh M, Ichiki T, Takeshita A: Importance of monocyte chemoattractant protein-1 pathway in neointimal hyperplasia after periarterial injury in mice and monkeys. *Circ Res* 2002, 90:1167–1172
  26. Zhang YJ, Rutledge BJ, Rollins BJ: Structure/activity analysis of human monocyte chemoattractant protein-1 (MCP-1) by mutagenesis: identification of a mutated protein that inhibits MCP-1-mediated monocyte chemotaxis. *J Biol Chem* 1994, 269:15918–15924
  27. Proost P, Struyf S, Couvreur M, Lenaerts JP, Conings R, Menten P, Verhaert P, Wuyts A, Van Damme J: Posttranslational modifications affect the activity of the human monocyte chemotactic proteins MCP-1 and MCP-2: identification of MCP-2(6–76) as a natural chemokine inhibitor. *J Immunol* 1998, 160:4034–4041
  28. Gong JH, Ratkay LG, Waterfield JD, Clark-Lewis I: An antagonist of monocyte chemoattractant protein 1 (MCP-1) inhibits arthritis in the MRL-lpr mouse model. *J Exp Med* 1997, 186:131–137
  29. Naito M, Umeda S, Yamamoto T, Moriyama H, Umezumi H, Hasegawa G, Usuda H, Shultz LD, Takahashi K: Development, differentiation, and phenotypic heterogeneity of murine tissue macrophages. *J Leukoc Biol* 1996, 59:133–138
  30. Hagerty RD, Salzman DL, Kleinert LB, Williams SK: Cellular proliferation and macrophage populations associated with implanted expanded polytetrafluoroethylene and polyethyleneterephthalate. *J Biomed Mater Res* 2000, 49:489–497
  31. Gong JH, Clark-Lewis I: Antagonists of monocyte chemoattractant protein 1 identified by modification of functionally critical NH<sub>2</sub>-terminal residues. *J Exp Med* 1995, 181:631–640
  32. Zhang Y, Rollins BJ: A dominant negative inhibitor indicates that monocyte chemoattractant protein 1 functions as a dimer. *Mol Cell Biol* 1995, 15:4851–4855
  33. McNally AK, DeFife KM, Anderson JM: Interleukin-4-induced macrophage fusion is prevented by inhibitors of mannose receptor activity. *Am J Pathol* 1996, 149:975–985
  34. Saginario C, Qian HY, Vignery A: Identification of an inducible surface molecule specific to fusing macrophages. *Proc Natl Acad Sci USA* 1995, 92:12210–12214
  35. Yamao T, Noguchi T, Takeuchi O, Nishiyama U, Morita H, Hagiwara T, Akahori H, Kato T, Inagaki K, Okazawa H, Hayashi Y, Matozaki T, Takeda K, Akira S, Kasuga M: Negative regulation of platelet clearance and of the macrophage phagocytic response by the transmembrane glycoprotein SHPS-1. *J Biol Chem* 2002, 277:39833–39839
  36. Saginario C, Sterling H, Beckers C, Kobayashi R, Solimena M, Ullu E, Vignery A: MFR, a putative receptor mediating the fusion of macrophages. *Mol Cell Biol* 1998, 18:6213–6223
  37. Han X, Sterling H, Chen Y, Saginario C, Brown EJ, Frazier WA, Lindberg FP, Vignery A: CD47, a ligand for the macrophage fusion receptor, participates in macrophage multinucleation. *J Biol Chem* 2000, 275:37984–37992
  38. Sterling H, Saginario C, Vignery A: CD44 occupancy prevents macrophage multinucleation. *J Cell Biol* 1998, 143:837–847
  39. Bonnema H, Popa ER, Van Timmeren MM, Van Wachem PB, De Leij LF, Van Luyn MJ: Distribution patterns of the membrane glycoprotein CD44 during the foreign-body reaction to a degradable biomaterial in rats and mice. *J Biomed Mater Res* 2003, 64A:502–508
  40. van Luyn MJ, Khouw IM, van Wachem PB, Blaauw EH, Werkmeister JA: Modulation of the tissue reaction to biomaterials: II. The function of T cells in the inflammatory reaction to crosslinked collagen implanted in T-cell-deficient rats. *J Biomed Mater Res* 1998, 39:398–406
  41. Iizuka T, Kohgo T, Marks Jr SC: Foreign body giant cell induction in the CSF-1-deficient osteopetrotic (op/op) mouse. *Tissue Cell* 2002, 34:103–108
  42. Brodbeck WG, Patel J, Voskerician G, Christenson E, Shive MS, Nakayama Y, Matsuda T, Ziats NP, Anderson JM: Biomaterial adherent macrophage apoptosis is increased by hydrophilic and anionic substrates in vivo. *Proc Natl Acad Sci USA* 2002, 99:10287–10292